Folding of an Abridged β-Lactamase†

Javier Santos,[‡,§] Leopoldo G. Gebhard,[‡,§] Valeria A. Risso,[‡] Raul G. Ferreyra,[‡,§] Juan P. F. C. Rossi,[§,||] and Mario R. Ermácora*[,‡,§]

Departamento de Ciencia y Tecnología, Universidad Nacional de Quilmes, Roque Sáenz Peña 180, (1876) Bernal, Buenos Aires, Argentina, Consejo Nacional de Investigaciones Científicas y Técnicas, Rivadavia 1917, (1033) Ciudad Autónoma de Buenos Aires, Argentina, and Facultad de Farmacia y Bioquímica, Universidad de Buenos Aires, Junín 956, (1113) Ciudad Autónoma de Buenos Aires, Argentina

Received October 7, 2003; Revised Manuscript Received December 4, 2003

ABSTRACT: The effects of C-terminal truncation on the equilibrium folding transitions and folding kinetics of *B. licheniformis exo small* β−lactamase (ES-βL) have been measured. ES-βL lacking 19 residues (ES-$\beta L^{C\Delta 19}$) has no enzymic activity. Deletion of the last 14 residues produces ES-$\beta L^{C\Delta 14}$, which is 0.1% active. The enzyme lacking nine residues (ES-$\beta L^{C\Delta 9}$) is nearly fully active, has native optical and hydrodynamic properties, and is protease resistant, a distinguishing feature of the wild-type enzyme. Although ES-$\beta L^{C\Delta 9}$ folds properly, it does so 4 orders of magnitude slower than ES-βL, making possible the isolation and characterization of a compact intermediate state (I_P ES-$\beta L^{C\Delta 9}$). Based on the analysis of folding rates and equilibrium constants, we propose that equilibrium between I_P ES-$\beta L^{C\Delta 9}$ and other intermediate slow folding. Residues removed in ES-$\beta L^{C\Delta 9}$ and ES-$\beta L^{C\Delta 14}$ are helical and firmly integrated into the enzyme body through many van der Waals interactions involving residues distant in sequence. The results suggest that the deleted residues play a key role in the folding process and also the existence of a modular organization of the protein matrix, at the subdomain level. The results are compared with other examples of this kind in the folding literature.

Although amino acid sequence determines protein conformation (*1*), the correspondence between sequence and structure is not exact. Some amino acid replacements are well tolerated, whereas others are disruptive (*2*−*5*). Also, we have observed that deletion of the last three residues of fatty-acid-binding protein (IFABP[1]) causes the protein to fold into a compact state lacking tertiary structure (*6*), whereas an internal deletion of 17 residues fails to interfere with the formation of native IFABP (*7*). These considerations led us to propose that the conformational information content varies widely along the polypeptide chain and that the formation of compact states and the fine adjustment of tertiary interactions can be uncoupled by specific residue deletion (*6*). However, in the case of truncated IFABP, a small population of native state molecules might have escaped detection by the optical and hydrodynamic probes utilized. To avoid this obstacle, and assuming that catalytic activity is the best criterion of native structure, we now have chosen to test the proposal with *exo small* β-lactamase (ES-βL), whose biological activity, unlike that of IFABP, can be determined readily and unambiguously even at trace levels.

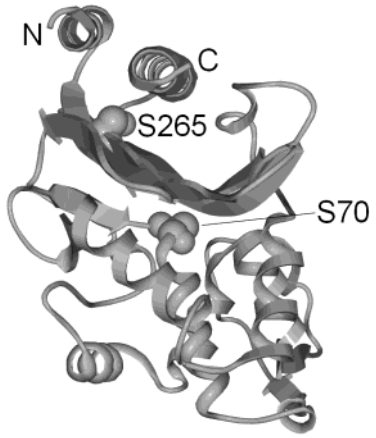

FIGURE 1: Ribbon diagram of ES-βL. The upper half of the molecule comprises the $\alpha + \beta$ domain built with pieces of C- and N-terminal sequences. The lower half depicts the α domain, which is built entirely from middle-part sequence. Ser 70 (at the catalytic site) and Ser 265 (replaced by cysteine in S265C ES-βL) are represented in space-filling mode.

The three-dimensional (3D) structure of ES-βL is known to high-resolution (see PDB entries 2BLM and 4BLM) (*8*, *9*). This 265-residue protein has no cysteine, and it is organized in two noncontinuous domains (Figure 1): the $\alpha + \beta$ domain is formed by a central, five-stranded β sheet covered by three superficial α-helices; the other domain is a globular array of helical elements. The interface between the two domains harbors the catalytic site.

† This work was supported by grants from CONICET, Agencia Nacional de Promoción Científica y Técnica, Universidad Nacional de Quilmes, Third World Academy of Sciences, and Fundación Antorchas.

* To whom correspondence should be addressed. Tel.: +54 (114) 365 7100. Fax: +54 (114) 365 7132. E-mail: ermacora@mail.unq.edu.ar.

‡ Universidad Nacional de Quilmes.

§ Consejo Nacional de Investigaciones Científicas y Técnicas.

|| Universidad de Buenos Aires.

[1] Abbreviations: ES-βL, *B. licheniformis* ES-β-lactamase; N, native state; U, unfolded state; I, intermediate state; ES-$\beta L^{C\Delta n}$, ES-βL lacking *n* residues from the C-terminus; native ES-$\beta L^{C\Delta 9}$, native monomeric ES-$\beta L^{C\Delta 9}$; I_P ES-$\beta L^{C\Delta 9}$, partially folded compact state of ES-$\beta L^{C\Delta 9}$; SEC, size exclusion chromatography; CD, circular dichroism; SDS−PAGE, sodium dodecyl sulphate polyacrylamide gel electrophoresis; GdmCl, guanidinium chloride; ANS, 1-anilinonaphthalene-8-sulfonate; DTNB, 5,5′-dithiobis-(nitrobenzoic acid); λ_{max}, wavelength spectroscopic maximum; K_D, dissociation constant.

10.1021/bi0358162 CCC: $27.50
Published on Web 01/22/2004

The general folding properties of ES-βL are also known (*10*). It is a stable protein (~8 kcal/mol), with a remarkable resistance to proteolysis, which populates several equilibrium partially folded states. Kinetic measurements indicated that ES-βL folds in few minutes, with multiple phases. This protein is a good model for medium-size, non-two-state folders because its tendency toward irreversible aggregation is limited. In addition, its catalytic activity can be used to assess folding in vitro or to select active mutants in vivo.

Since most protein termini are on the protein surface (*11*), moderate chain truncation produces no internal cavities that may complicate the interpretation of folding experiments. Moreover, the underlying surface exposed upon truncation can be readily evaluated using molecular models, and if balanced in terms of hydrophobicity, it leaves only the specific tertiary contacts removed as the cause of observed effects on folding. Thus, truncation seems to be a valuable tool to identify clusters of conformational information crucial for folding (*6*, *12*).

We prepared ES-$\beta L^{C\Delta 9}$, ES-$\beta L^{C\Delta 14}$, and ES-$\beta L^{C\Delta 19}$, variants of lactamase truncated nine, fourteen, and nineteen residues from the C-terminus, respectively. It is noteworthy that the last four C-terminal residues of ES-βL were not observed in the electronic density map and are presumed disordered (*9*). Examining the molecular model, the deletions were designed to assess the contribution to global folding of long-range interactions established by the sixteen-residue C-terminal α helix with two flanking helices and the core β sheet (Figure 1). The residues deleted in each variant were chosen as to eliminate gradually interactions with different parts of the enzyme body. As a control, in ES-$\beta L^{C\Delta 19}$, the C-terminal α helix was eliminated, removing all the interactions under study. In ES-$\beta L^{C\Delta 14}$, the helix was reduced by ~2/3, removing most of the interactions with the adjacent helices and the β sheet underneath. In ES-$\beta L^{C\Delta 9}$, only five helical residues were removed, eliminating most interhelical contacts while preserving the contacts with the β sheet.

ES-$\beta L^{C\Delta 19}$ preparations had no enzymic activity, suggesting that the deletion of 19 residues impedes native folding. However, ES-$\beta L^{C\Delta 14}$ exhibits low levels of enzymic activity, which implies that some of the ES-$\beta L^{C\Delta 14}$ molecules are able to reach a native or nativelike fold. On the other hand, ES-$\beta L^{C\Delta 9}$ is competent to reach a native state with nearly full enzymic activity, but it does so quite slowly, allowing the observation of an intermediate state almost at will. A preliminary characterization of this intermediate state is presented, along with evidence showing that the last nine residues of ES-βL have a key role facilitating rapid folding and helping to avoid kinetic traps and aggregation.

MATERIALS AND METHODS

General Details. Mass spectra were acquired with a VG Quatro II (VG Biotech, Altrinchan, U.K.) instrument. Data fitting was done with Solver (Microsoft Excel 2000). Protein purity was estimated by SDS−PAGE (*13*). Molecular graphics were prepared using Insight II (MSI, San Diego, CA) and Swiss-PDB Viewer (Glaxo Wellcome Experimental Research). Absorption spectra were obtained with a Shimadzu UV160A spectrophotometer (Tokyo, Japan). Enzymic activity was determined at 25 °C in 50 mM sodium phosphate, pH 7.0 supplemented with 1.5 μM bovine serum albumin, and 0.5 mg/mL benzylpenicillin (*10*, *14*). Limited trypsinolysis was performed in 100 mM sodium phosphate, pH 7.0 (buffer A), for 5 min, at 20 °C, and a weight ratio protease:β-lactamase of 1:100. Accessible surface area was calculated using ACCESS (M. D. Handschumacher and F. M. Richards, Yale University, 1983). Analytical size-exclusion chromatography (SEC) was carried out at 4 or 20 °C with a Superose 12 column (Pharmacia, Uppsala, Sweden), equilibrated and eluted with buffer A, and UV detection at 280 nm. Stokes' radii (R_S) were calculated as described (*10*). Preparative SEC was carried out at 4 °C on a Sephacryl S-100 HR column (2.6 × 90 cm; Pharmacia, Uppsala, Sweden) equilibrated and eluted with 150 mM sodium phosphate pH 7.0.

Preparation of β-Lactamase Variants. ES-βL expression vector, *pELB3* was previously described (*10*); *c*DNAs for ES-$\beta L^{C\Delta 9}$, ES-$\beta L^{C\Delta 14}$, ES-$\beta L^{C\Delta 19}$, S265C ES-βL, and S265C ES-$\beta L^{C\Delta 9}$ were prepared from *pELB3* by PCR mutagenesis (*15*) with *Pfu* DNA polymerase and appropriate primers. PCR products were ligated into the *XbaI*/*BamHI* site of *pET9a*. Transformed *Escherichia coli* BL21 (DE3) cells were cultured in Luria Bertani medium at 37 °C to A_{600} nm ~ 1.0, induced with 1 mM IPTG (3 h), and harvested by centrifugation.

ES-βL and S265C ES-βL were purified as described (*10*). To isolate truncated ES-βL variants, inclusion bodies (*16*) were treated with solubilization buffer (6.5 M urea, 25 mM phosphoric acid, 5 mM glycine, pH 3.5), solubilized proteins were resolved with a fast flow S−Sepharose column (1.5 × 7.0 cm) and a 100 mL, 0−500 mM NaCl gradient in solubilization buffer. Fractions containing pure, truncated β-lactamase were pooled and stored at −20 °C. In the case of S265C ES-$\beta L^{C\Delta 9}$, 10 mM DTT was added to solubilization and chromatography buffers. When required, urea was exchanged to GdmCl by dialysis or SEC. The identity of all produced lactamase was confirmed by mass spectrometry.

Optical Studies. CD spectra were obtained at 22 °C on a Jasco J-810 spectropolarimeter (Jasco Corporation, Japan). Instrument settings and data processing were previously described (*17*). CD buffer was 10 mM sodium phosphate, 100 mM sodium fluoride, pH 7.0. Protein concentration was 8−15 and 1.5 μM for near- and far-UV, respectively.

Steady-state fluorescence was recorded at 20 °C on a K2 ISS spectrofluorometer (ISS, Champaign, IL). Excitation was at 295 nm with 8 nm bandwidth. Quantum yield (Q) was calculated using tryptophan as the standard ($Q = 0.14$). Protein concentration was 4 μM in buffer A.

Chemical Modifications. Cross-linking with 0−0.5% glutaraldehyde (Fluka, Switzerland) or 0−1.5 mM disuccinimidiyl glutarate (Pierce, Rockford, IL) was carried out for 30 min at 4 °C. Protein concentration was 0.2 mg/mL in 100 mM sodium phosphate. The reaction was terminated by adding 50 mM Tris-HCl, pH 7.5, and followed by SDS−PAGE. Thiol accessibility was determined using 5,5'-dithiobis-(2-nitrobenzoic acid) (DTNB) (*18*) at 25 °C in 75 mM sodium phosphate, 250 mM sodium sulfate, pH 6.0.

Folding Equilibrium. Lactamases were incubated 2 h at room temperature with 0−3.5 M GdmCl in buffer A. Tertiary structure probes were fluorescence (295 and 335 nm excitation and emission, respectively) and enzymic activity. Data processing was performed according to Santoro and Bolen (*19*).

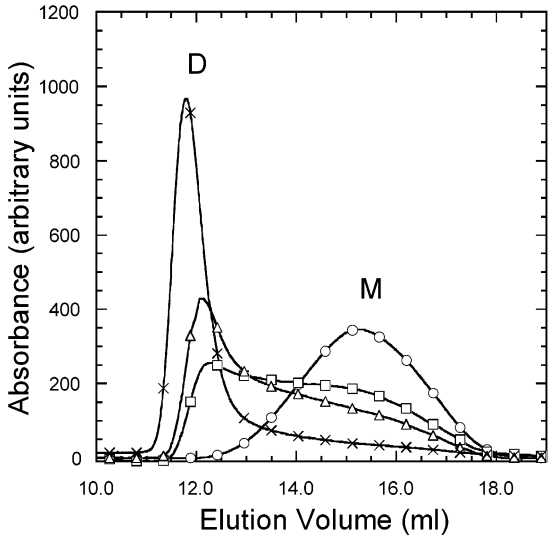

FIGURE 2: Dissociation equilibrium of I_P ES-$\beta L^{C\Delta 9}$. Analytical SEC was performed at 4 °C. Protein concentration in the column was 1.5 μM (○), 3.3 μM (□), 5.1 μM (△) and 28.4 μM (×). The total area under each chromatogram was normalized to the mass of protein injected.

Folding Kinetics. Lactamases were incubated 5 h with 5 M GdmCl in buffer A and diluted into buffer A to 0.05−1.5 M denaturant. For unfolding, dilution was from buffer A to the same buffer supplemented with 1.5−5 M GdmCl. In both cases, temperature was 20 °C, and final protein concentration was 0.3−30 μM. Aliquots were withdrawn at regular intervals, and enzymic activity was measured as described (*10*). In short, samples were assayed with the cell thermostated at 10 °C (ES-βL) or 20 °C (ES-$\beta L^{C\Delta 9}$), absorbance at 240 nm was recorded every 0.1 s during 15-second intervals, and the slope was used to calculate activity. Mixing and reading were completed in less than 30 s; thus, no significant error was introduced due to refolding during measurement. Refolding of ES-$\beta L^{C\Delta 9}$ was also monitored by SEC; time point samples were injected into a Superose 12 column equilibrated with buffer A at 4 °C.

RESULTS

Protein Expression, Purification, and Refolding. ES-βL variants were expressed at 80−250 mg/L of culture and purified to 95−98% homogeneity. ES-βL and S265C ES-βL are produced soluble in *E. coli* and were purified in the native state. ES-$\beta L^{C\Delta 9}$, ES-$\beta L^{C\Delta 14}$, and ES-$\beta L^{C\Delta 19}$ form inclusion bodies and were purified in concentrated urea. Upon refolding by overnight dialysis or dilution, ES-$\beta L^{C\Delta 19}$ is inactive, but ES-$\beta L^{C\Delta 9}$ and ES-$\beta L^{C\Delta 14}$ yield preparations with 10% and 0.1% specific activity relative to wild-type ES-βL (it is noteworthy that native ES-βL can be unfolded by urea and quantitatively refolded as above yielding fully active protein; not shown).

The refolding products obtained by overnight dialysis at 4 °C were subjected to analytical and preparative SEC. ES-$\beta L^{C\Delta 9}$ elutes in three main fractions: monomer (R_S = 25.4 ± 0.6 Å), dimer (R_S = 31.2 ± 0.6 Å), and higher-order aggregates. ES-$\beta L^{C\Delta 14}$ and ES-$\beta L^{C\Delta 19}$ behave similarly, except for the absence of monomeric fractions (not shown). The specific activity of monomeric ES-$\beta L^{C\Delta 9}$ is 76% ± 5% (relative to ES-βL), and K_M are 0.18 ± 0.05 and 0.16 ± 0.03 mM, for ES-βL and ES-$\beta L^{C\Delta 9}$, respectively (n = 3). Dimers and higher-order aggregates lack enzymic activity. Moreover, all fractions but ES-βL and monomeric ES-$\beta L^{C\Delta 9}$ are sensitive to proteolysis.

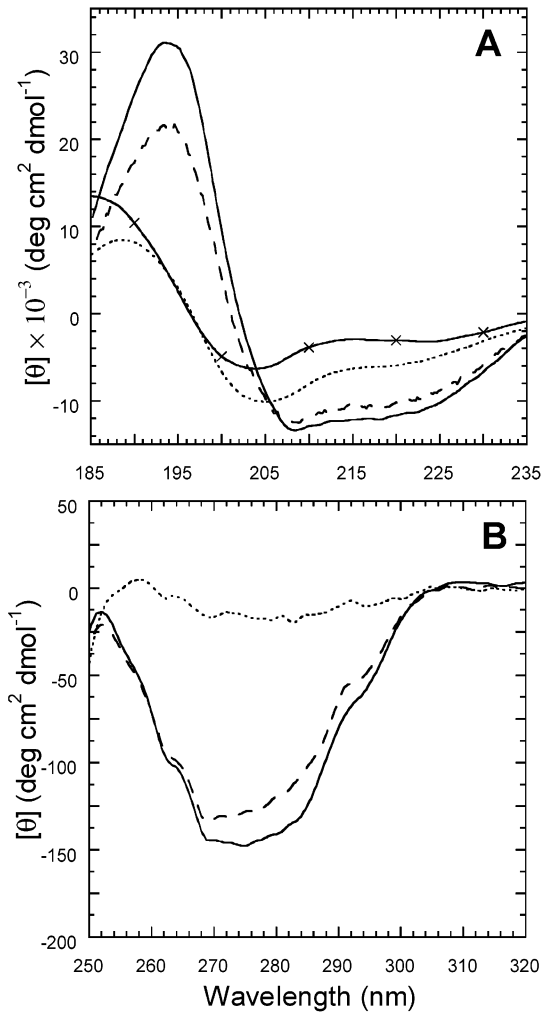

FIGURE 3: Circular dichroism spectra of ES-βL variants. (A) Far-UV spectra. Protein concentration was 1.5 μM protein in 10 mM sodium phosphate, 100 mM sodium fluoride, pH 7.0. (B) Near-UV. Protein concentration was 15 μM in buffer A. ES-βL, native ES-$\beta L^{C\Delta 9}$, and I_P ES-$\beta L^{C\Delta 9}$ are shown as solid (—), long dash (— —), and short dash (---), respectively. All measurements were at 20 °C, except for thermally unfolded ES-βL (—×—) whose spectrum was recorded at 80 °C.

Resistance to proteolysis is a distinguishing feature of native β-lactamase and strongly suggests that monomeric ES-$\beta L^{C\Delta 9}$ has a properly folded structure. Accordingly, the latter will be hereafter referred to as "native" ES-$\beta L^{C\Delta 9}$. Dimeric ES-$\beta L^{C\Delta 9}$ folds slowly into native ES-$\beta L^{C\Delta 9}$ (see below) and will be denominated I_P ES-$\beta L^{C\Delta 9}$ ("productive" intermediate). A full characterization of ES-$\beta L^{C\Delta 14}$ and ES-$\beta L^{C\Delta 19}$ will be presented elsewhere; herein, we focus on the properties of ES-$\beta L^{C\Delta 9}$.

General Properties of I_P ES-$\beta L^{C\Delta 9}$. Its ability of forming a dimer was corroborated by two additional lines of evidence. First, in chemical cross-linking experiments, ES-βL and I_P ES-$\beta L^{C\Delta 9}$ produces traces and ~30% of covalently stabilized dimer, respectively; whereas higher-order aggregates of ES-$\beta L^{C\Delta 9}$ give products that barely migrate in SDS−PAGE (not shown). Second, in analytical SEC, below ~10 μM, I_P ES-$\beta L^{C\Delta 9}$ dissociates into two peaks, in a concentration-

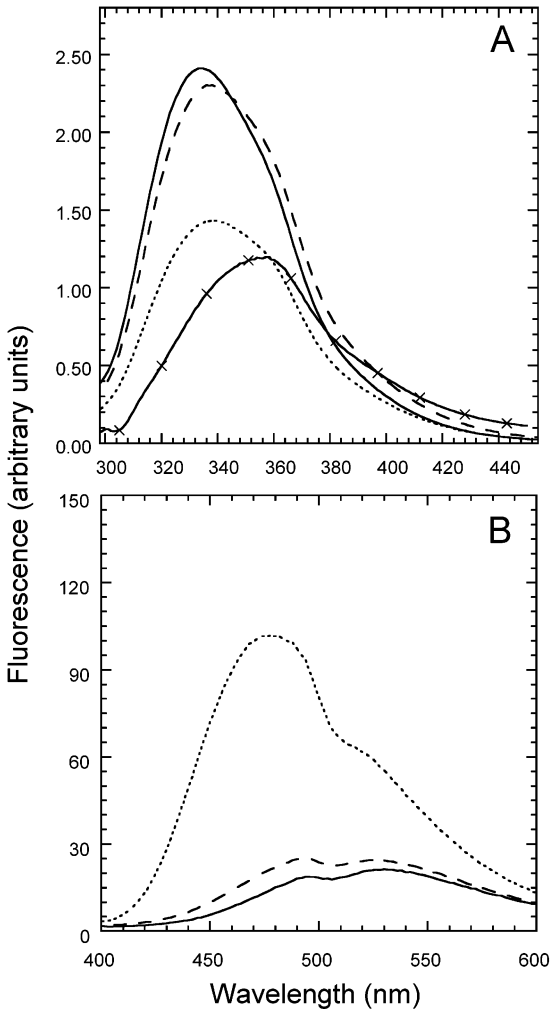

FIGURE 4: (A) Fluorescence spectra of ES-βL variants. Protein concentration was 4 μM in buffer A. Excitation was at 295 nm, and the data were normalized for absorption at 290 nm. ES-βL, native ES-βL$^{C\Delta9}$, and I$_P$ ES-βL$^{C\Delta9}$ are shown as solid (—), long dash (— —), and short dash (---), respectively. Fluorescence of GdmCl-unfolded ES-βL (—×—) was measured in 5 M GdmCl. (B) ANS binding to native ES-βL$^{C\Delta9}$ and I$_P$ ES-βL$^{C\Delta9}$ followed by fluorescence. Protein concentration was 3 μM in buffer A. Excitation was at 350 nm. Emission spectra of 53 μM ANS in the presence of native ES-βL$^{C\Delta9}$, I$_P$ ES-βL$^{C\Delta9}$ or in the absence of protein are shown as long dash (— —), short dash (---) and solid (—), respectively.

dependent equilibrium (Figure 2). Interestingly, these two peaks have no enzymic activity, suggesting that transiently monomeric I$_P$ ES-βL$^{C\Delta9}$ differs from stably monomeric, native ES-βL$^{C\Delta9}$.

CD and fluorescence spectra (Figures 3 and 4) indicated that I$_P$ ES-βL$^{C\Delta9}$ is a molten globule: (a) It has a far-UV rotatory power, compatible with a reduction in secondary structure. (b) Its near-UV CD spectrum is flat and featureless suggesting absence of tertiary structure. (c) It has native λ_{max} of fluorescence emission, but a greatly lowered quantum yield. (d) It binds ANS. On the other hand, the optical properties of native ES-βL$^{C\Delta9}$ are nearly identical to those of wild-type ES-βL.

Folding Equilibrium. GdmCl-induced unfolding curves (Figure 5) indicated that ES-βL is a very stable protein (ΔG^0_u = 8.4 kcal mol^{-1}; m = 6.6 kcal mol^{-1} M^{-1}; C_m = 1.3 M). Although activity and fluorescence curves are nearly superimposable, a slight inflection at the beginning of the

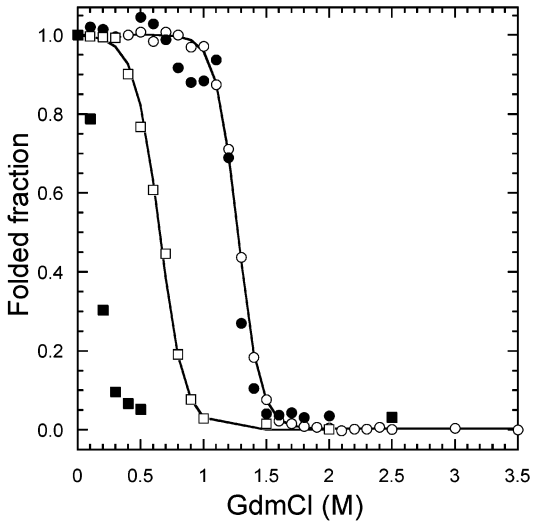

FIGURE 5: Equilibrium unfolding curves. ES-βL (circles) and native ES-βL$^{C\Delta9}$ (squares) in buffer A supplemented with GdmCl. Folded fraction was estimated by fluorescence (empty symbols) and enzymic activity (filled symbols).

main activity transition suggests a perturbation of the two-state equilibrium. Indeed, R_S measurements at low denaturant concentrations demonstrated the existence of a slightly expanded native state in equilibrium with the unfolded species (not shown). Incidentally, compactness is dependent on GdmCl concentration also across the transition, and after the main transition at least one more equilibrium intermediate is populated, the state "H", which is characterized by a shift in the maximum of the emission between 1.5 and 3 M GdmCl (*10*, *20*).

Native ES-βL$^{C\Delta9}$ has fair thermodynamic stability (ΔG^0_u = 3.8 kcal mol^{-1}; m = 5.8 kcal mol^{-1} M^{-1}; C_m = 0.6 M). However, ES-βL$^{C\Delta9}$ activity is lost in a nonsigmoidal fashion, well before major changes in fluorescence occur (Figure 5). Adding sodium sulfate shifts the fluorescence curve toward higher denaturant concentrations but does not increase the initial specific activity (not shown). At GdmCl concentrations of 0.5 M, ES-βL$^{C\Delta9}$ populates another conformationally distinct state, nearly as compact as the native one, which is inactive but, unlike I$_P$ ES-βL$^{C\Delta9}$, possess nativelike fluorescence intensity and λ_{max}. The properties of this state are being investigated and will be reported elsewhere.

Folding Kinetics. Refolding of ES-βL and ES-βL$^{C\Delta9}$, upon dilution from 5 to 0.05 M GdmCl, was monitored by enzymic activity (Figure 6). For ES-βL, amplitude and relaxation time are 100% and 1.7 min, respectively, whereas for ES-βL$^{C\Delta9}$ these parameters are 30% and 589 min. Adding 250 mM sodium sulfate doubles the refolding yield and causes a 5-fold increase in the rate constant of ES-βL$^{C\Delta9}$. Interestingly, the additive has no effect on the kinetic of ES-βL. Conversion of dimeric I$_P$ ES-βL$^{C\Delta9}$ into native monomeric ES-βL$^{C\Delta9}$, followed by analytical SEC (Figure 7), has a relaxation time of 575 min: thus, acquisition of enzymic activity and formation of the native monomer occur at approximately the same rate. It should be emphasized that, since a transient monomeric and inactive form of I$_P$ ES-βL$^{C\Delta9}$ can be isolated by SEC (Figure 2), dissociation of dimeric I$_P$ ES-βL$^{C\Delta9}$ into monomers occurs faster than formation of native ES-βL$^{C\Delta9}$.

To further investigate the effect of the dimer—monomer equilibrium on the rate of folding, the kinetics experiment

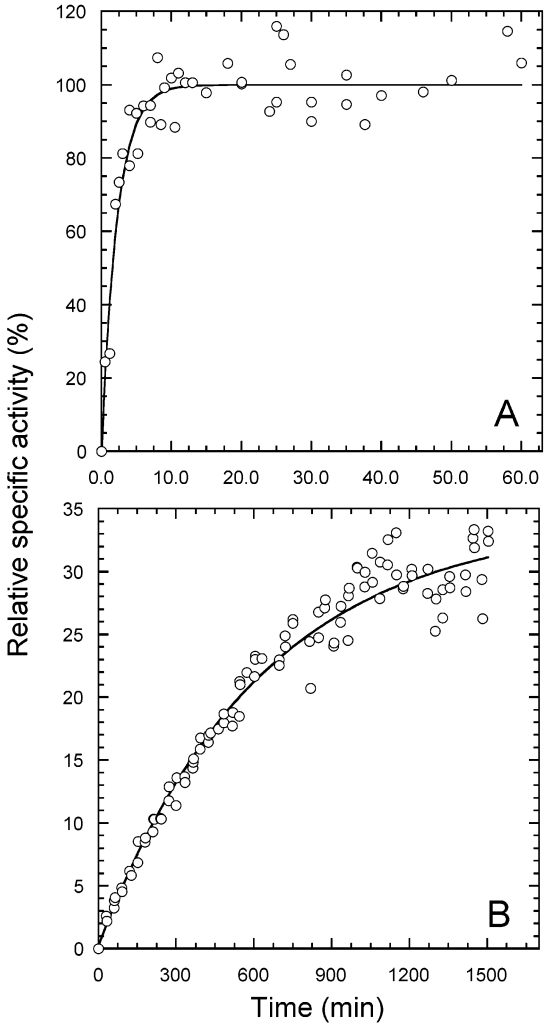

FIGURE 6: Refolding kinetics. ES-βL (A) and ES-$\beta L^{C\Delta 9}$ (B) were unfolded at 20 °C by a 5-h incubation in 5 M GdmCl and then refolded by 1:100 dilution into buffer A. Catalytic activity is relative to the specific activity of the respective native pure proteins.

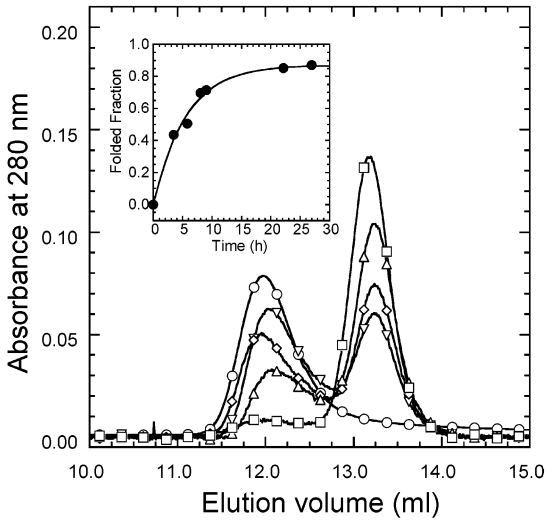

FIGURE 7: Time course of ES-$\beta L^{C\Delta 9}$ refolding followed by SEC. Protein concentration was 8 μM. Conditions were as described in Figure 6. At selected times, 0 (○), 3 (▽), 6 (◇), 8 (△), and 22 h (□), the reaction was terminated by cooling to 4 °C and injection into a Superose 12 column equilibrated at the same temperature. Folded fraction (Inset) was calculated as the fraction of area eluting under the monomer peak (~13.2 mL).

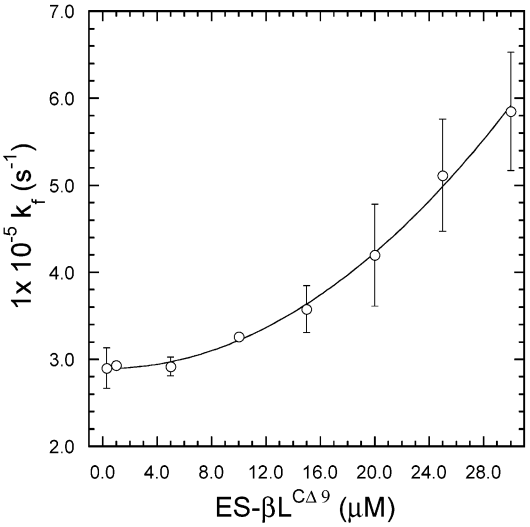

FIGURE 8: Protein concentration dependency of ES-$\beta L^{C\Delta 9}$ rate of folding. The experiment reported in Figure 6 was performed varying protein concentration in the refolding mixture.

was carried out at different protein concentrations (Figure 8). The rate of folding does not increase as protein concentration decreases below 10 μM, as it would if the dissociation of the dimer were an obligatory rate-limiting step (i.e., dimer ↔ monomer → N). Instead, the rate increases slightly with concentration above 10 μM. Since dissociation depends on protein concentration, it can be shown that the results in Figure 8 can only be explained by placing dimeric I_P ES-$\beta L^{C\Delta 9}$ "on pathway" (or in equilibrium with an on-pathway intermediate) in the route to N (i.e., monomer↔ dimer→N). Furthermore, the rate reaches a plateau different from zero at very low protein concentration. If monomeric I_P ES-$\beta L^{C\Delta 9}$ were unable to fold into N without dimerizing, the rate would extrapolate to zero. This shows that both monomeric and dimeric I_P ES-$\beta L^{C\Delta 9}$ are able fold to N. Thus, the dimerization of I_P ES-$\beta L^{C\Delta 9}$ is an epiphenomenon that does not obstruct the analysis of the effect of truncation on the mechanism folding. In fact, the following kinetics experiments were done at protein concentrations such as only monomeric I_P ES-$\beta L^{C\Delta 9}$ was significantly populated.

Chevron Plots. A number of reasons led us to monitor enzymic activity rather that tryptophan fluorescence in folding kinetic experiments. First, previous results showed that ES-βL folding kinetics monitored by fluorescence is multiphasic and complex (*10*). Second, the very slow rate of folding of ES-$\beta L^{C\Delta 9}$ and parallel formation of aggregates makes comparative kinetics measurements by fluorescence problematic due to instrumental drift and light scattering artifacts. Third, the existence of partially folded states of ES-βL with nativelike fluorescence properties, as noted above, introduces uncertainty about the truly native nature of folding products. In unfolding kinetics experiments, however, fluorescence measurements were feasible and easier to interpret. Thus, correspondence between fluorescence change and activity loss during unfolding could be ascertained in control experiments.

Folding rates at 20 °C, as a function of GdmCl concentration, are shown in Figure 9 A. Native and unfolded samples (0 and 5 M GdmCl respectively) were diluted to the indicated denaturant concentrations and assayed for enzymic activity as a function of time. Since dilution and transfer to the quartz

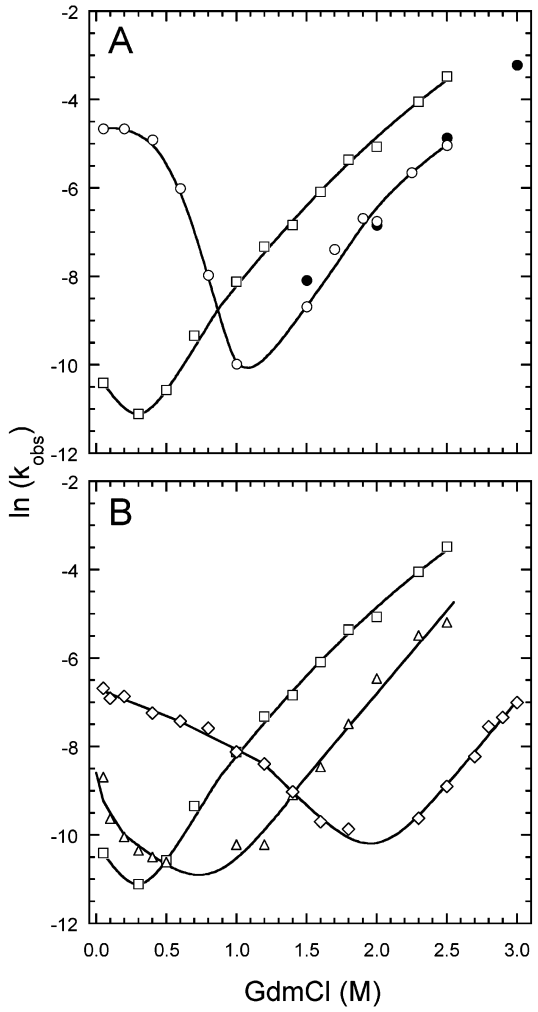

FIGURE 9: Chevron Plots. Unfolding and refolding rates of ES-βL and ES-$\beta L^{C\Delta 9}$ as a function of GdmCl were determined in buffer A at 20 °C. The reaction was followed by enzymic activity (empty symbols) and fluorescence emission (solid circles). Panel A: ES-βL (○) and ES-$\beta L^{C\Delta 9}$ (□). Panel B: the effect of sodium sulfate concentrations, 0.0 M (□), 0.25 M (△), and 1.0 M (◇), on ES-$\beta L^{C\Delta 9}$ folding is shown.

cuvette took ~15 s, only reactions with relaxation times larger than 20 s were measurable. Fortunately, this was not a limitation because all relaxation times are larger than 30 s.

Below 0.4 M GdmCl, ES-βL refolding rate is nearly constant with $\tau = 105$ s. This "rollover" may have a number of explanations, including a change in the rate-limiting step and the transient accumulation of a folding intermediate (*21*). Also, since the dependence of the logarithm of folding rate on denaturant concentration is related to the difference in exposed surface between ground and transition states, it is possible that, under strongly native conditions, ES-βL folding involves a rate-limiting step with little or no change in surface area. The lack of effect of sodium sulfate (see above) is in agreement with this interpretation. Furthermore, in a previous work using similar conditions, we found that ES-βL regains native fluorescence with $\tau = 2.5$ ms (*10*). Thus, at low denaturant concentrations, the formation of the active site seems to occur in an already compact state in which Trp residues are shielded from solvent.

Between 0.6−2 M GdmCl, the plot for ES-βL exhibits the typical "V" shape of two-state folders, with the kinetics parameters listed in Table 1. There are a reasonable agreement between ΔG^0_u and m calculated from kinetics and equilibrium experiments. However, C_m calculated from kinetics is 1.0 M, whereas the value obtained from equilibrium is 1.3 M. The discrepancy may be due to fluorescence being less sensitive to the denaturant than activity (see Figure 5). Moreover, $\beta_{N\rightarrow\ddagger}$ was 0.28, implying that the transition state is, in exposed surface area, closer to N than to U.

For ES-$\beta L^{C\Delta 9}$, a full comparison between equilibrium and kinetics was not possible because the refolding limb started close to zero denaturant concentration. Nevertheless, combining k_{obs} at nearly zero denaturant concentration and k^0_u obtained by extrapolation from the right arm of the plot, it can be estimated that ΔG^0_u is about 0.5 kcal mol^{-1}, much lower than the ΔG^0_u calculated from equilibrium experiments. Discrepancy between transitions monitored by fluorescence and activity is likely due to the presence of inactive but compact partially folded states and departure from the two-state mechanism at equilibrium.

At the lowest denaturant concentrations, ES-$\beta L^{C\Delta 9}$ acquires in few seconds the fluorescence features of I_P ES-$\beta L^{C\Delta 9}$ (not shown). On the other hand, the transformation of I_P ES-$\beta L^{C\Delta 9}$ into active monomer has a relaxation time of ~10 h. Thus, late folding involves the very slow transformation of an already compact nonnative state into the compact native state. Nevertheless, m_f values calculated from the Chevron plot, both in absence and in the presence of sodium sulfate, suggest that crossing the activation barrier involves a large change in molecular accessible surface. Further evidence of this is the ~30-fold increase in k^0_f of ES-$\beta L^{C\Delta 9}$ in the presence of 1 M sodium sulfate (Figure 9 B). Since I_P ES-$\beta L^{C\Delta 9}$ is nearly as compact as native ES-$\beta L^{C\Delta 9}$, it seems unlikely that it were the last intermediate before the transition state. To account for this fact, we propose that I_P ES-$\beta L^{C\Delta 9}$ must unfold before progressing in the folding pathway.

At denaturant concentrations above C_m, partially folded states should be less stable than U, and the measured kinetics of unfolding is likely to be from N to U. In support of this assumption, SEC experiments at 1 M GdmCl exhibit only N and U ES-$\beta L^{C\Delta 9}$ (not shown). Given that, within experimental error, the slope of the right arm of the plot is the

Table 1: Kinetics Parameters for Folding (20 °C)[a]

	k^0_u (s^{-1})	k^0_f (s^{-1})	m_u (kcal mol^{-1} M^{-1})	m_f (kcal mol^{-1} M^{-1})	m_{kin}[b] (kcal mol^{-1} M^{-1})	ΔG^0_u (kcal mol^{-1})	$\beta_{N\rightarrow\ddagger}$[c]
ES-bL	1.2×10^{-6}	2.9×10^{-1}	2.0	5.2	7.3	7.2	0.3
ES-$\beta L^{C\Delta 9}$	6.4×10^{-6}	3.0×10^{-5}	2.0	–	–	0.8[d]	–

[a] The transition was monitored by enzymic activity (see Figures 3 and 5), and Chevron plot data close to midpoint of the transition were fitted to kinetics equations (*26*). All rates were from the extrapolation to zero denaturant of data from the "V-shaped" part of the graph, except k^0_f for ES-$\beta L^{C\Delta 9}$, which is the observed folding rate in 50 mM GdmCl. [b] $m_{kin} = m_u + m_f$. [c] $\beta_{N\rightarrow\ddagger} = m_u/(m_u + m_f)$. [d] Calculated as $\Delta G^0_u = -RT \ln(k^0_u/k^0_f)$.

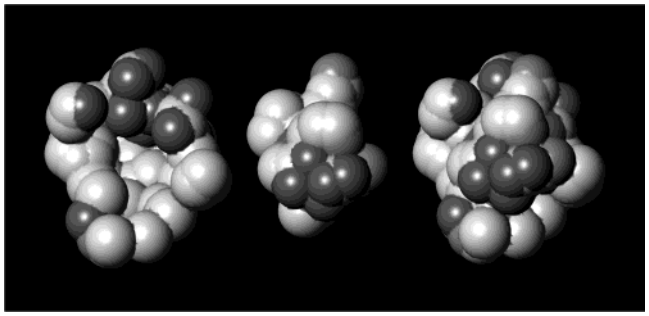

FIGURE 10: Docking of the ES-βL C-terminal helix. Left, surface below residues 282−295. Middle, residues 282−295. Right, complex between the residues 282−295 and ES-βL. Dark gray identifies oxygen atoms, nitrogen is represented in intermediate gray, and the clearer atoms are carbons.

same for ES-βL and ES-βL$^{C\Delta9}$ and that the exposed surface of N should also be nearly the same for both variants, their N → ‡ transition should involve similar change in exposed area. Therefore, for ES-βL$^{C\Delta9}$, the transition state should be relatively compact, closer to N than to U, similarly to what was described above for ES-βL.

Cys Mutants. To determine whether the helical C-terminus is occluding the underlying β structure in native ES-βL$^{C\Delta9}$ and I$_P$ ES-βL$^{C\Delta9}$, Ser 265, which is completely buried at the interface between the two secondary structure elements, was replaced by cysteine (Figure 1), and solvent accessibility of the mutants single thiol was assessed with DTNB (*18*). Native S265C ES-βL is unreactive, whereas S265C ES-βL unfolded in GdmCl reacts with the same rate as free β−mercaptoethanol (not shown). Clear-cut results were obtained with S265C ES-βL$^{C\Delta9}$: the native, enzymatically active species is unreactive and I$_P$ ES-βL$^{C\Delta9}$ reacted as β-mercaptoethanol.

DISCUSSION

Role of Helix 11 in Structure. Helix 11 is at the surface of the $\alpha + \beta$ domain, flanked by helices 1 and 10, and covering the β-sheet underneath (Figure 1). ES-βL$^{C\Delta19}$, which lacks helix 11, has a folding defect so severe that, even using the extremely sensitive lactamase assay, we fail to detected native state.

In ES-βL$^{C\Delta14}$, deletion of ∼2/3 of helix 11 exposes a new core surface much more hydrophobic than the original (76 vs 50% non polar; Figure 10). Besides, 86 van der Waals contacts (2.5−4.5 Å) are removed; of which 50 are at the hydrophobic interface between helices 1, 10, and 11, and the rest join helix 11 to the β-sheet underneath. The residues removed in ES-βL$^{C\Delta14}$ are closely packed and firmly integrated into the body of ES-βL. Furthermore, most of the tertiary contacts established by helix 11 are of the long-range type, closing loops of ∼30, ∼65, and ∼250 residues. Thus, a priori, on the basis of the marginal stability of folded proteins and in the principal role assigned to long-range interactions in the mechanism of folding, one would consider this truncation as firm candidate to abort completely productive folding. Yet ES-βL$^{C\Delta14}$ has 0.1% of the wild-type specific activity. This implies that some of ES-βL$^{C\Delta14}$ molecules successfuly solved the folding problem and managed to build the active site by properly positioning the interface between the two domains and most of the N-terminal elements of secondary structure. This remarkable feat implies that residues 282−295 of ES-βL, although optimize folding and stabilize the native state, are not essential from a structural point of view.

Role of Residues 287−295 in Folding Kinetics. Removal of one-and-a-half turns of helix 11 and the last four disordered residues yields ES-βL$^{C\Delta9}$, a molecule that folds into a monomeric state with fair yield, has catalytic parameters similar to those of the wild-type enzyme, and is resistant to proteolysis. The peptide removed in ES-βL$^{C\Delta9}$ participates in most of the interactions with the underlying β sheet and in only one of the interhelical contacts enumerated above. Almost perfect catalysis means accurate positioning of the interface between the two domains. Resistance to proteolysis, a distinctive feature of wild-type ES-βL, implies nativelike dynamic and accessibility of the entire polypeptide backbone. Further proof of the right packing of the shortened helix 11 was obtained by chemical modification of the single Cys mutant, S265C ES-βL$^{C\Delta9}$, which clearly demonstrated that the remains of helix 11 occlude the β sheet underneath.

Despite their low impact on the structure of the native state, residues 287−295 seem to affect dramatically the rate of folding: ES-βL$^{C\Delta9}$ folds 10^4 times slower than ES-βL. Whereas ES-βL forms fully active monomers within seconds, ES-βL$^{C\Delta9}$ forms I$_P$ ES-βL$^{C\Delta9}$, a highly compact molten globule that evolves very slowly to native ES-βL$^{C\Delta9}$ and higher-order aggregates.

Neither burst nor lag phases of enzymic activity were observed for I$_P$ ES-βL$^{C\Delta9}$, which suggests a single track to native state and points to the latter−or an intermediate in fast equilibrium with it−as the ground state for the rate-limiting step in folding. I$_P$ ES-βL$^{C\Delta9}$ participates in a dimer−monomer equilibrium; however, monomeric I$_P$ ES-βL$^{C\Delta9}$ folds to native ES-βL$^{C\Delta9}$ even more slowly than dimeric I$_P$ ES-βL$^{C\Delta9}$, implying that the slow rate of folding is not the consequence of the tendency of I$_P$ ES-βL$^{C\Delta9}$ to dimerize. Moreover, sodium sulfate dependence of the folding and unfolding rates indicates that I$_P$ ES-βL$^{C\Delta9}$ should expand further before crossing the kinetic barrier, implying that the rate-limiting intermediate for folding is a product of I$_P$ ES-βL$^{C\Delta9}$ and not I$_P$ ES-βL$^{C\Delta9}$ itself.

Since I$_P$ ES-βL$^{C\Delta9}$ and unfolded ES-βL both generate a native lactamase, their folding pathway must overlap to some extent. It seems very unlikely that two large polypeptides differing only nine overhanging residues would sample entirely different subsets of conformations and converge only at the final product. Therefore, we propose that either, there is an equivalent to I$_P$ ES-βL$^{C\Delta9}$ on the folding pathway of ES-βL or I$_P$ ES-βL$^{C\Delta9}$ is an off-pathway intermediate that is connected to the main route of ES-βL folding. We cannot distinguish between these two possibilities with the present data.

During folding, a relatively fast equilibrium between I$_P$ ES-βL$^{C\Delta9}$ and the rate-limiting intermediate could be established. The latter seems similar to the state I described for TEM β-lactamase (*22*), which is on the path to native state at a branching point to aggregation. It is worth mentioning that other proteins have been found to populate transiently associated intermediates (*23*−*25*).

By lowering the effective concentration of the ground state, equilibrium between I$_P$ ES-βL$^{C\Delta9}$ and the rate-limiting intermediate provides the simpler explanation for the slow refolding of ES-βL$^{C\Delta9}$ (*21*, *26*). However, slower folding may

also result from a change in the mechanism of folding and/or an increase in the energy of the transition state relative to U. A change in mechanism seems less likely because the slope of the unfolding arm of the Chevron plot is the same within experimental error for ES-βL and I_P ES-$\beta L^{C\Delta 9}$, which is an indication of similarity in the exposed area of their respective transition states. Moreover, adding sodium sulfate shifted the curves to higher denaturant concentrations, confirmed that the plot is indeed V shaped in the proximity to the midpoint and provided slopes compatible with a similar folding mechanism for ES-βL and ES-$\beta L^{C\Delta 9}$ (Figure 9). On the other hand, simulations of Chevron plots, based on estimates of the equilibrium constant as a function of denaturant concentration and reasonable changes in exposed area for the transition state, suggest that the difference in the folding rate of I_P ES-$\beta L^{C\Delta 9}$ and ES-βL may be only partly explained by an equilibrium between I_P ES-$\beta L^{C\Delta 9}$ and the rate-limiting intermediate, and therefore the truncation seems to increase the energy of transition state relative to U (M.R.E. and J.S., unpublished results).

Information Content of the Polypeptide Chain. The existence of native proteins lacking part of their sequences bears relevance on fundamental aspects of folding. Recently, we suggested that conformational information may vary widely along the chain (*6*). The results presented herein shed further light on the subject. Since the last nine residues of ES-βL can be eliminated without impeding folding, they carry no essential information for nonlocal 3D structure. Most importantly, they are not unique in this regard. A truncated ES-βL has been prepared that lacks 14 N-terminal residues and still exhibits substantial enzymic activity (J.S. et al., unpublished results), and a variant of the homologous β-lactamase from *Staphylococcus aureus* lacking a nonterminal segment of 16 residues is very similar to the wild-type enzyme, as evidenced by X-ray crystallography (*27*).

In line with the findings for ES-βL, protein segments having no essential information for the native state seems to be rather common. Several other examples were listed by Kumar et al. (*28*). These examples and the findings of this work suggest that the long-range conformational information is limited to few residues or confined to specific regions of the sequence.

CONCLUSIONS

ES-$\beta L^{C\Delta 9}$ differs from ES-βL in lacking nine C-terminal residues; however, the two variants fold into similar native structures and show similarly compact transition states. Thus, late-folding events cannot be very different for these variants. Since ES-$\beta L^{C\Delta 9}$ folds 10^4 fold slower than ES-βL, the deleted residues must be crucial for rapid and efficient folding. ES-$\beta L^{C\Delta 9}$ populates transiently I_P ES-$\beta L^{C\Delta 9}$, a molten globule that can be isolated and studied by conventional optical probes. Equilibrium between I_P ES-$\beta L^{C\Delta 9}$ and another intermediate on-pathway offers a logical explanation for the observed kinetics differences. Nevertheless, preliminary calculations indicate that a direct effect of the deleted residues on the relative energy of the transition state cannot be discarded.

Finally, the results presented herein identify the last nine residues of ES-βL as devoid of long-range conformational information. Examples from the literature suggest that this may be a rather common phenomenon. This implies that at least parts of the protein matrix might have a modular organization, built upon docking of small building blocks with little transfer of conformational information between them. Perhaps, if further research confirms this concept, the problem of predicting the structure of the native state from the sequence would be simplified.

ACKNOWLEDGMENT

We thank Prof. Anthony Fink for providing us with the lactamase gene and many suggestions on this protein. We are indebted to Dr. R. Baldwin for the critical reading of the manuscript.

REFERENCES

1. Anfinsen, C. B. (1973) Principles that govern the folding of protein chains, *Science 181*, 223−230.
2. Palzkill, T., and Botstein, D. (1992) Probing β-lactamase structure and function using random replacement mutagenesis, *Proteins 14*, 29−44.
3. Craig, S., Hollecker, M., Creighton, T. E., and Pain, R. H. (1985) Single amino acid mutations block a late step in the folding of beta-lactamase from Staphylococcus aureus, *J. Mol. Biol. 185*, 681−687.
4. Hughson, F. M., Barrick, D., and Baldwin, R. L. (1991) Probing the stability of a partly folded apomyoglobin intermediate by site-directed mutagenesis, *Biochemistry 30*, 4113−4118.
5. Shortle, D., and Meeker, A. K. (1989) Residual structure in large fragments of staphylococcal nuclease: effects of amino acid substitutions, *Biochemistry 28*, 936−944.
6. Clerico, E. M., Peisajovich, S. G., Ceolin, M., Ghiringhelli, P. D., and Ermacora, M. R. (2000) Engineering a compact non-native state of intestinal fatty acid-binding protein, *Biochim. Biophys. Acta 1476*, 203-218.
7. Cistola, D. P., Kim, K., Rogl, H., and Frieden, C. (1996) Fatty acid interactions with a helix-less variant of intestinal fatty acid-binding protein, *Biochemistry 35*, 7559−7565.
8. Moews, P. C., Knox, J. R., Dideberg, O., Charlier, P., and Frère, J. M. (1990) Beta-lactamase of *Bacillus licheniformis* 749/C at 2 A resolution, *Proteins 7*, 156−171.
9. Knox, J. R., and Moews, P. C. (1991) Beta-lactamase of *Bacillus licheniformis* 749/C. Refinement at 2 A resolution and analysis of hydration, *J. Mol. Biol. 220*, 435−455.
10. Frate, M. C., Lietz, E. J., Santos, J., Rossi, J. P., Fink, A. L., and Ermacora, M. R. (2000) Export and folding of signal-sequenceless *Bacillus licheniformis* beta-lactamase in *Escherichia coli*, *Eur. J. Biochem. 267*, 3836−3847.
11. Miller, S., Janin, J., Lesk, A. M., and Chothia, C. (1987) Interior and surface of monomeric proteins, *J. Mol. Biol. 196*, 641−656.
12. Neira, J. L., and Fersht, A. R. (1999) Exploring the folding funnel of a polypeptide chain by biophysical studies on protein fragments, *J. Mol. Biol. 285*, 1309−1333.
13. Schägger, H., and von Jagow, G. (1987) Tricine-sodium dodecyl sulfate-polyacrylamide gel electrophoresis for the separation of proteins in the range from 1 to 100 kDa, *Anal. Biochem. 166*, 368−379.
14. Jansson, J. A. T. (1965) A direct spectrophotometric assay for penicillin β-lactamase (penicillinase), *Biochim. Biophys. Acta*. *99*, 171−172.
15. Higuchi, R. (1989) in *PCR Technology. Principles and Applications for DNA Amplification* (Herlich, H. A., Ed.) pp 61−70., Stockton Press, New York.
16. Jessen, T. H., Komiyama, N. H., Tame, J., Pagnier, J., Shih, D., Luisi, B., Fermi, G., and Nagai, K. (1994) Production of human hemoglobin in *Escherichia coli* using cleavable fusion protein expression vector, *Methods Enzymol. 231*, 347−364.
17. Clérico, E. M., and Ermácora M., R. (2001) Tryptophan Mutants of Intestinal Fatty Acid Binding Protein: UV Absorption and Circular Dichroism Studies, *Arch. Biochem. Biophys. 395*, 215−224.

18. Jiang, N., and Frieden, C. (1993) Intestinal fatty acid binding protein: characterization of mutant proteins containing inserted cysteine residues, *Biochemistry 32*, 11015−11021.
19. Santoro, M. M., and Bolen, D. W. (1992) A test of the linear extrapolation of unfolding free energy changes over an extended denaturant concentration range, *Biochemistry 31*, 4901−4907.
20. Robson, B., and Pain, R. H. (1976) The mechanism of folding of globular proteins. Equilibria and kinetics of conformational transitions of penicillinase from *Staphylococcus aureus* involving a state of intermediate conformation, *Biochem. J. 155*, 331−344.
21. Baldwin, R. L. (1996) On pathway versus off pathway folding intermediates, *Fold. Des. 1*, R1−8.
22. Zahn, R., and Plückthun, A. (1994) Thermodynamic partitioning model for hydrophobic binding of polypeptides by GroEL. II. GroEL recognizes thermally unfolded mature beta-lactamase, *J. Mol. Biol. 242*, 165−174.
23. Ganesh, C., Zaidi, F. N., Udgaonkar, J. B., and Varadarajan, R. (2001) Reversible formation of on-pathway macroscopic aggregates during the folding of maltose binding protein, *Protein. Sci. 10*, 1635−1644.
24. Brems, D. N., and Havel, H. A. (1989) Folding of bovine growth hormone is consistent with the molten globule hypothesis, *Proteins 5*, 93−95.
25. Brems, D. N., Plaisted, S. M., Dougherty, J. J., Jr., and Holzman, T. F. (1987) The kinetics of bovine growth hormone-folding are consistent with a framework model, *J. Biol. Chem. 262*, 2590−2596.
26. Fersht, A. (1999) *Structure and Mechanism in Protein Science: A Guide to Enzyme Catalysis and Protein Folding*, New York.
27. Banerjee, S., Pieper, U., Kapadia, G., Pannell, L. K., and Herzberg, O. (1998) Role of the omega-loop in the activity, substrate specificity, and structure of class A β-lactamase, *Biochemistry 37*, 3286−3296.
28. Fischer, K. F., and Marqusee, S. (2000) A rapid test for identification of autonomous folding units in proteins, *J. Mol. Biol. 302*, 701−712.

BI0358162